J Toxicol Pathol 2021; 34: 223–230

Original Article

Ion channel mRNA distribution and expression in the sinoatrial node and right atrium of dogs and monkeys

Tomoya Sano[1]*, Hironobu Yasuno[1], and Takeshi Watanabe[1]

[1] Drug Safety Research and Evaluation, Takeda Pharmaceutical Company Limited, 26-1 Muraoka-Higashi 2-Chome, Fujisawa, Kanagawa 251-8555, Japan

Abstract: There are limited data on the gene expression profiles of ion channels in the sinoatrial node (SAN) of dogs and monkeys. In this study, the messenger RNA (mRNA) expression profiles of various ion channels in the SAN of naïve dogs and monkeys were examined using RNAscope® *in situ* hybridization and compared with those in the surrounding right atrium (RA) of each species. Regional-specific Cav1.3 and HCN4 expression was observed in the SAN of dogs and monkeys. Additionally, HCN1 in dogs was only expressed in the SAN. The expression profiles of Cav3.1 and Cav3.2 in the SAN and RA were completely different between dogs and monkeys. Dog hearts only expressed Cav3.2; however, Cav3.1 was detected only in monkeys, and the expression score in the SAN was slightly higher than that in the RA. Although Kir3.1 and NCX1 in dogs were equally expressed in both the SAN and RA, the expression scores of these genes in the SAN of monkeys were slightly higher than those in the RA. The Kir3.4 expression score in the SAN of dogs and monkeys was also slightly higher than that in the RA. The mRNA expression scores of Kv11.1/ERG and KvLQT1 were equally observed in both the SAN and RA of dogs and monkeys. HCN2 was not detected in dogs and monkeys. In summary, we used RNAscope to demonstrate the SAN-specific gene expression patterns of ion channels, which may be useful in explaining the effect of pacemaking and/or hemodynamic effects in nonclinical studies. (DOI: 10.1293/tox.2020-0089; J Toxicol Pathol 2021; 34: 223–230)

Key words: *in situ* hybridization, sinoatrial node, right atrium, ion channels, dogs, monkeys

Introduction

Cardiovascular (CV) safety risk in drug development is a principal concern because adverse CV effects can result in serious safety issues and termination of drug development. Definitive CV safety pharmacology studies are generally performed in large, nonrodent species, such as dogs and monkeys. To interpret the mode of action of CV toxicity, it is important to understand the target gene expression profiles of impulse conducting systems. However, in general, published gene and protein expression data in nonclinical species are derived from the whole heart, and limited information specific to impulse conducting systems (e.g., the sinoatrial node [SAN] and/or atrioventricular nodes) is available for both dogs and monkeys.

The heart beat is regulated by an electric impulse, and this cardiac action potential is initiated by the SAN under physiological conditions[1]. This cardiac impulse in the SAN is initially mediated by a sodium influx via hyperpolarization-activated cyclic nucleotide-gated cation channels (HCN1, 2, and 4). Thereafter, depolarization occurs progressively via T-type calcium channels (Cav3.1 and 3.2), and L-type calcium channels (Cav1.2 and 1.3)[2, 3]. Repolarization of the cardiac action potential occurs via the inactivation of L-type calcium currents and the opening of potassium channels, such as IKr (Kv11.1/hERG) and IKs (KCNQ1/KvLQT1) in the SAN. The blockade of IKr (Kv11.1/hERG), which is a key component in repolarization, is known to prolong the action potential and QT intervals due to delayed repolarization[2]. In addition to these key ion channels, the messenger RNA (mRNA) expression levels of acetylcholine-activated K+ current, IKACh (Kir3.1 and 3.4), and sodium-calcium exchanger 1 (NCX1) are also known to regulate the cardiac action potential[3].

In this study, we investigated the gene expression profiles of various ion channels in the SAN and surrounding right atrium (RA) using formalin-fixed, paraffin-embedded (FFPE) samples from naïve beagle dogs and cynomolgus monkeys.

Materials and Methods

Three naïve beagle dogs (one male and two females) and three cynomolgus monkeys (one male and two females) were used in this study. The animals were individually

Received: 22 December 2020, Accepted: 2 April 2021
Published online in J-STAGE: 18 April 2021
*Corresponding author: T Sano (E-mail: tomoya.sano@takeda.com)

housed in metal cages set on racks in animal rooms under the following controlled conditions: temperature of 22–27 °C for monkeys or 20–26 °C for dogs, a 12 h light/dark cycle, and humidity at 40–80%. The animals were fed a solid diet and had free access to water. The dogs and monkeys were euthanized at 28 months and 5–6 years old, respectively, by exsanguination under anesthesia and subjected to complete necropsy. The hearts were fixed in 10% v/v neutral buffered formalin, embedded in paraffin, sectioned, and stained with hematoxylin and eosin to identify the SANs. The experimental procedures were approved by the Institutional Animal Care and Use Committee of Shonan Health Innovation Park (Fujisawa, Japan).

RNAscope® in situ hybridization

RNAscope is a universal assay for RNA transcript detection. The probe design algorithm and novel probe concept (a double-Z design) improve cross-hybridization between target probes as well as assay specificity[4]. In this study, mRNA levels of ion channels from FFPE heart tissues, including those from the RA and SAN, were detected using RNAscope. RNAscope staining was conducted using the Leica Bond RX system (Leica Biosystems, Wetzlar, Germany) according to the automated ISH protocol for RNAscope 2.5 LS Reagent Kit–Brown (ACDBio, Newark, CA, USA). Two RNAscope positive control probes from ACDBio were used in this study: positive control probe monkey and dog ubiquitin C (Mfa-UBC; Cat No. 461338, Accession No. XM_005572601.1 and Cl-UBC; Cat No. 409858, Accession No. XM_847967.3, respectively) and one negative control probe, dihydrodipicolinate reductase (bacterial DapB; Cat No. 312038, Accession No. EF191515). Information regarding the target probes is presented in Table 1. The dots of each target gene were uniformly observed in each cell or region in the present study. Semiquantitative evaluation for the positive control and target probes was conducted in the entire part of each region (SAN and RA): 0: no staining; 1+ (low): 1–3 dots/cell; 2+ (mild): 4–10 dots/cell; 3+ (moderate): 10–15 dots/cell; and 4+ (high): > 15 dots/cell (not observed in this study). Each specimen was microscopically examined by a pathologist, and a reviewing pathologist confirmed the individual scores. Based on results from the vendor-recommended positive control staining (UBC; Cat No. 409858 for dogs and 461338 for monkeys), the quality of the FFPE samples was confirmed to be suitable for RNAscope (mean score ≥ 3+). No staining was observed in the negative control (DapB); therefore, the assay met the acceptance criteria for the qualification of all samples. There were no apparent differences in the target mRNA expression scores between individual animals and between the sexes of either species.

mRNA quantification

Real-time reverse transcription polymerase chain reaction (RT-PCR) analyses were conducted to determine the levels of dog HCN2, CACNA1G (Cav3.1), CACNA1H (Cav3.2), and glyceraldehyde 3-phosphate dehydrogenase (GAPDH), which was used to normalize the data. These genes were selected to clarify the accuracy of RNAscope data because there was a discrepancy between the present data and the previous information[5, 6].

Total RNA was isolated from the FFPE heart sections adjacent to the sections analyzed by RNAscope *in situ* hybridization from one female dog using the RNeasy® FFPE Kit (Qiagen, Tokyo, Japan). For complementary DNA (cDNA) synthesis, 1 µg of total RNA was reverse transcribed using the SuperScript® VILOTM cDNA Synthesis Kit (Thermo Fisher Scientific Inc., Tokyo, Japan) and GeneAmp® PCR System 9700 thermal cycler (Life Technologies, Inc., Carlsbad, CA, USA). Real-time RT-PCR (TaqMan) analysis for the relative determination of mRNA levels was performed using the standard curve method. TaqMan reactions were performed in optical 384-well reaction plates by adding 10 µL of a reaction mixture comprising 1 µL of cDNA solution, 5 µL of TaqMan Universal Master Mix II, no UNG (Thermo Fisher Scientific Inc., Tokyo, Japan), 0.5 µL of TaqMan gene expression assay primers (Applied Biosystems, Foster City, CA, USA), and 3.5 µL of autoclaved water. A 10 µL aliquot of an RT-PCR sample prepared as described above was subsequently added to each well. The reactions were performed in triplicate, and the temperature profile was 95 °C for 10 min, followed by 40 cycles of 95 °C for 15 s and 60 °C for 1 min. The samples were amplified, read,

Table 1. RNAscope® target probe information

Target name	Gene symbol	Catalog No. [Dog/Monkey]	Accession No. [Dog/Monkey]
HCN1	*HCN1*	568498/568528	XM_850162.4/XM_005556858.2
HCN2	*HCN2*	5680508/568538	XM_014121847.2/XM_015440169.1
HCN4	*HCN4*	568518/568548	XM_022412726.1/XM_005559993.2
Cav1.2	*CACNA1C*	567648/567738	XM_022411432.1/XM_015430237.1
Cav1.3	*CACNA1D*	544908/544898	XM_014122083.2/XM_015446025.1
Cav3.1	*CACNA1G*	567658/567718	XM_022423104.1/XM_005583707.2
Cav3.2	*CACNA1H*	567668/567728	XM_014114721.2/XM_005590829.2
Kv11.1/ERG	*KCNH2*	587298/587338	NM_001003145.1/XM_005551163.1
KCNQ1/KvLQT1	*KCNQ1*	587308/587348	XM_022405121.1/XM_015435245.1
Kir3.1	*KCNJ3*	587318/587358	XM_545477.6/XM_005573205.2
Kir3.4	*KCNJ5*	587328/587368	XM_546402.6/XM_005580148.2
NCX1	*SLC8A1*	587278/587288	NM_001304962.1/XM_015433734.1

and analyzed using the *ABI PRISM* 7900HT Sequence Detection System and *ABI PRISM SDS 2.4* software (Applied Biosystems Japan, Tokyo, Japan). The cycle number (C_T) at which the fluorescence, generated by cleavage of the probe, exceeded the threshold was determined for each well. The C_T values of the genes were normalized against the C_T value of a housekeeping gene (GAPDH) amplified from the same RNA samples. Data are presented as $2^{-\Delta Ct}$ values to show the ratio to GAPDH. ΔCt was calculated as follows: $\Delta Ct = (Ct_{\text{gene of interest}} - Ct_{GAPDH})$. Additionally, we performed real-time RT-PCR analysis using commercially available RNA from a dog heart (DR-801; Zyagen, San Diego, CA, USA). The mRNA assay IDs are listed in Table 2.

Results

Microscopic examinations

Microscopically, the SAN was located near the crista terminalis. The monkey SAN was identified in the subendocardial region, whereas the canine SAN was observed in the epicardial side of the RA with the SAN artery (Fig. 1A and 1B). The SAN in both monkeys and dogs was characterized by glycogen-containing compact cardiomyocytes with a few interstitial fibrous matrices (Fig. 1C and 1D) compared to cardiomyocytes in the RA (Fig. 1E and 1F).

Table 2. mRNA assay IDs used for TaqMan reverse transcription polymerase chain reaction in a dog

Gene Symbol	Gene name	Assay ID
HCN2	hyperpolarization activated cyclic nucleotide gated potassium channel 2	Cf02735844_m1
CACNA1G	calcium channel, voltage-dependent, T type , alpha 1G subunit	Cf02723988_m1
CACNA1H	calcium channel, voltage-dependent, T type, alpha 1H subunit	Cf02693684_m1
GAPDH	glyceraldehyde-3-phosphate dehydrogenase	Cf04419463_gH

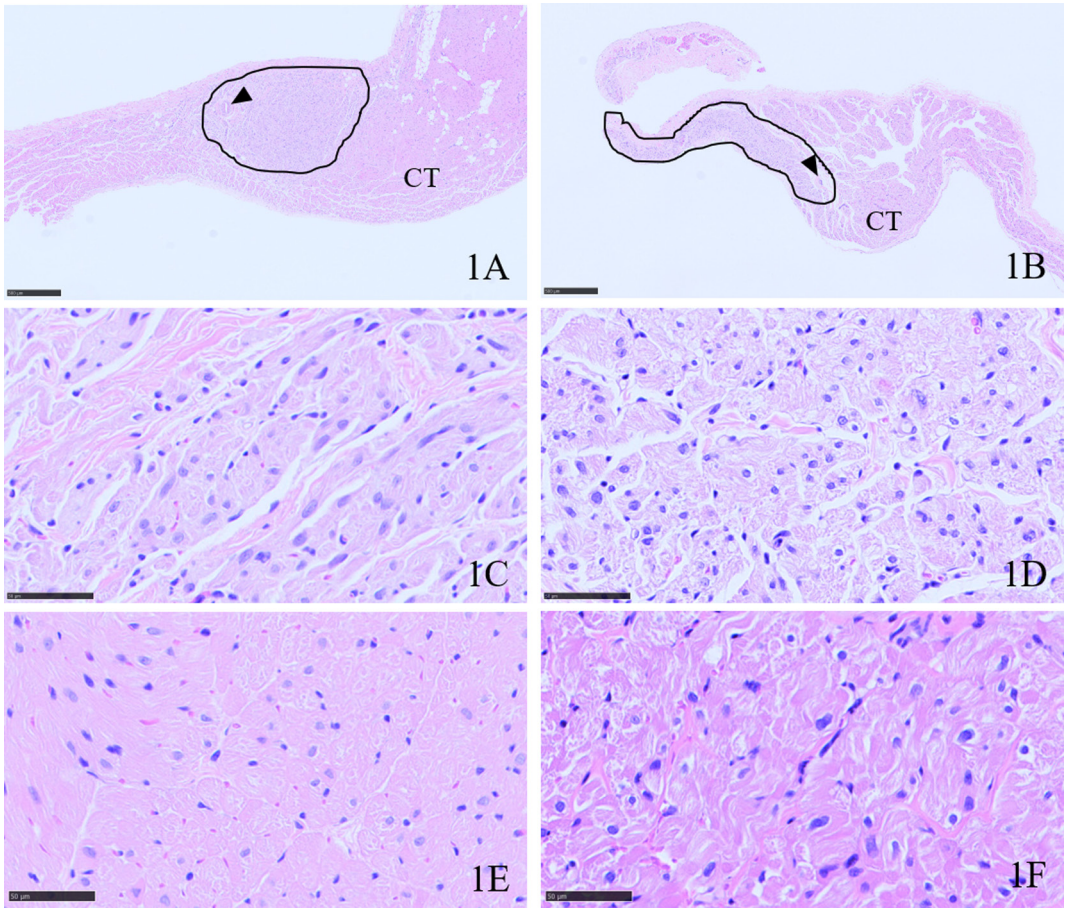

Fig. 1. Representative photos of monkey and dog hearts (hematoxylin and eosin staining). A: Low magnification figure of a dog heart (the black frame indicates the SAN region; bar: 1 mm), B: Low magnification figure of a monkey heart (the black frame indicates the SAN region; bar: 1 mm), C: High magnification of the SAN region in a dog (bar: 50 µm), D: High magnification of the SAN region in a monkey (bar: 50 µm), E: High magnification of the RA region in a dog (bar: 50 µm), F: High magnification of the RA region in a monkey (bar: 50 µm). Arrowheads indicate the SAN artery. SAN: sinoatrial node; RA, right atrium; CT: crista terminalis.

RNAscope in situ hybridization

Many of the targets showed punctate staining patterns in the cytoplasm, and some dots were also observed in the nucleus at various frequencies. The regional mRNA expression pattern or score for each target mRNA is shown in Fig. 2.

For hyperpolarization-activated cyclic nucleotide-gated channels (HCN1, 2, and 4), low to mild expression of HCN1 was confirmed in both the SAN and RA in monkeys (Fig. 3A and 3B), but mild expression of HCN1 was detected only in the SAN in dogs (Fig. 4A and 4B). HCN2 was not detected in either region in dogs or monkeys. Mild to moderate expression of HCN4 was confirmed in the SAN in both dogs and monkeys (Fig. 3C and 4C). Low expression of HCN4 in the RA was also noted in monkeys but not in dogs (Fig. 3D and 4D).

Regarding voltage-gated calcium channels (Cav1.2, 1.3, 3.1, and 3.2), the L-type voltage-gated calcium channel Cav1.2 was equally expressed in the SAN and RA, and the expression score was low to mild in both dogs and monkeys. In contrast, mild SAN-specific expression of Cav1.3 was noted in both dogs and monkeys (Figs. 3E, 3F, 4E, and 4F). The gene expression profiles of T-type voltage-gated calcium channels (Cav3.1 and 3.2) in the SAN and RA were completely different between dogs and monkeys (Fig. 5A–5H). Cav3.2 was equally expressed at low levels in the SAN and

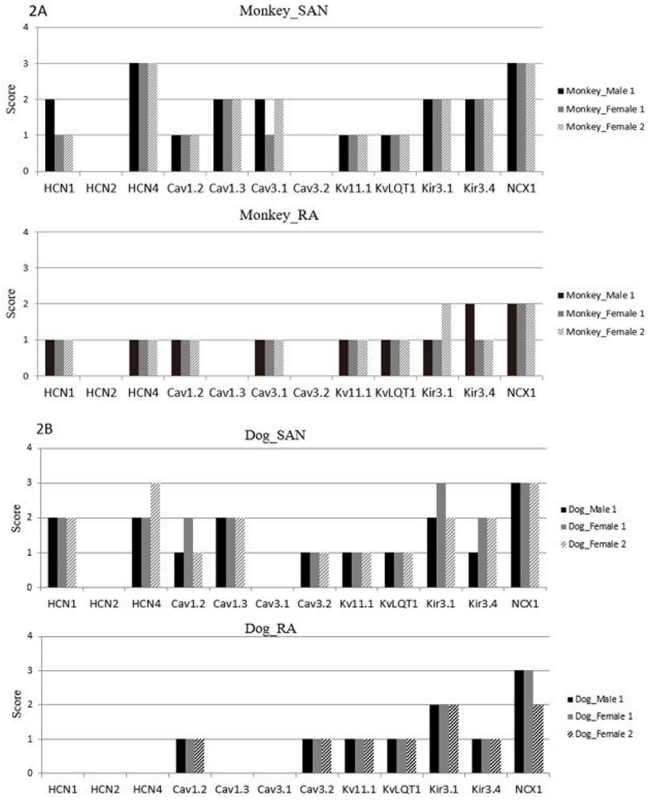

Fig. 2.

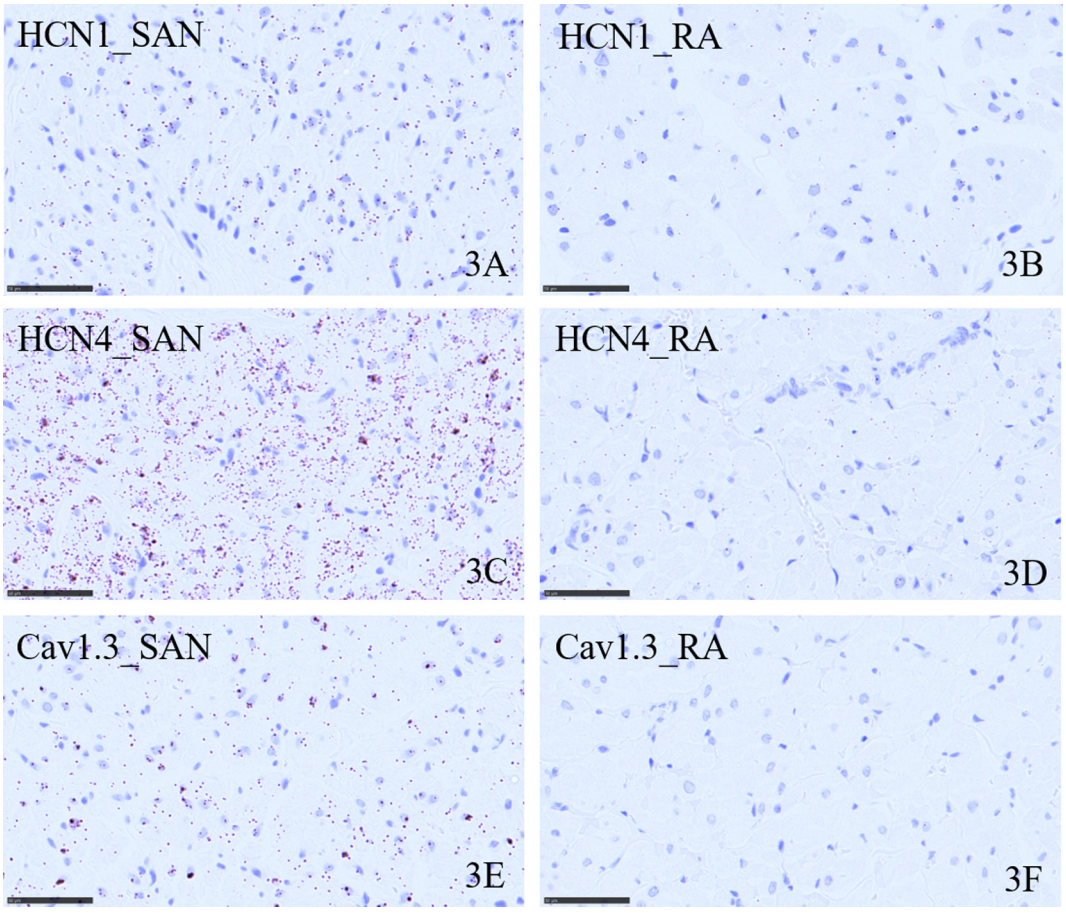

Fig. 3.

RA in dogs but not in monkeys. In contrast, low to mild expression of Cav3.1 was only noted in the SAN and RA in monkeys, and its expression score was slightly higher in the SAN.

In terms of voltage-gated potassium channels (Kv11.1/ERG, KvLQT1, Kir3.1, and Kir3.4), low expression levels of Kv11.1/ERG and KvLQT1 mRNAs were observed in both the SAN and RA, and there were no differences in expression patterns between the two regions and species. Kir3.1 mRNA was confirmed in the SAN and RA of monkeys (low to mild) and dogs (mild to moderate), and its expression score in the SAN was slightly higher than that in the RA in monkeys, although the scores were equivalent in dogs. Low to mild expression of Kir3.4 mRNA was observed in the SAN and RA of dogs and monkeys, and its expression score in the SAN was slightly higher than that in the RA.

For NCX1, mild to moderate expression of NCX1 in dogs and monkeys was noted in the SAN and RA. Although the NCX1 gene in dogs was equally expressed in both the SAN and RA, the expression of NCX1 in the SAN was slightly higher than that in the RA in monkeys.

Relative CACNA1G (Cav3.1), CACNA1H (Cav3.2), and HCN2 mRNA differences in dogs

The mRNA expression level of each target was lower than that of GAPDH (Fig. 6). The relative expression level of the Cav3.2 gene was higher than those of the Cav3.1 and HCN2 genes (Fig. 6). The trend in target mRNA expression levels using the FFPE sample of a female dog was comparable to that of a commercially available control RNA from

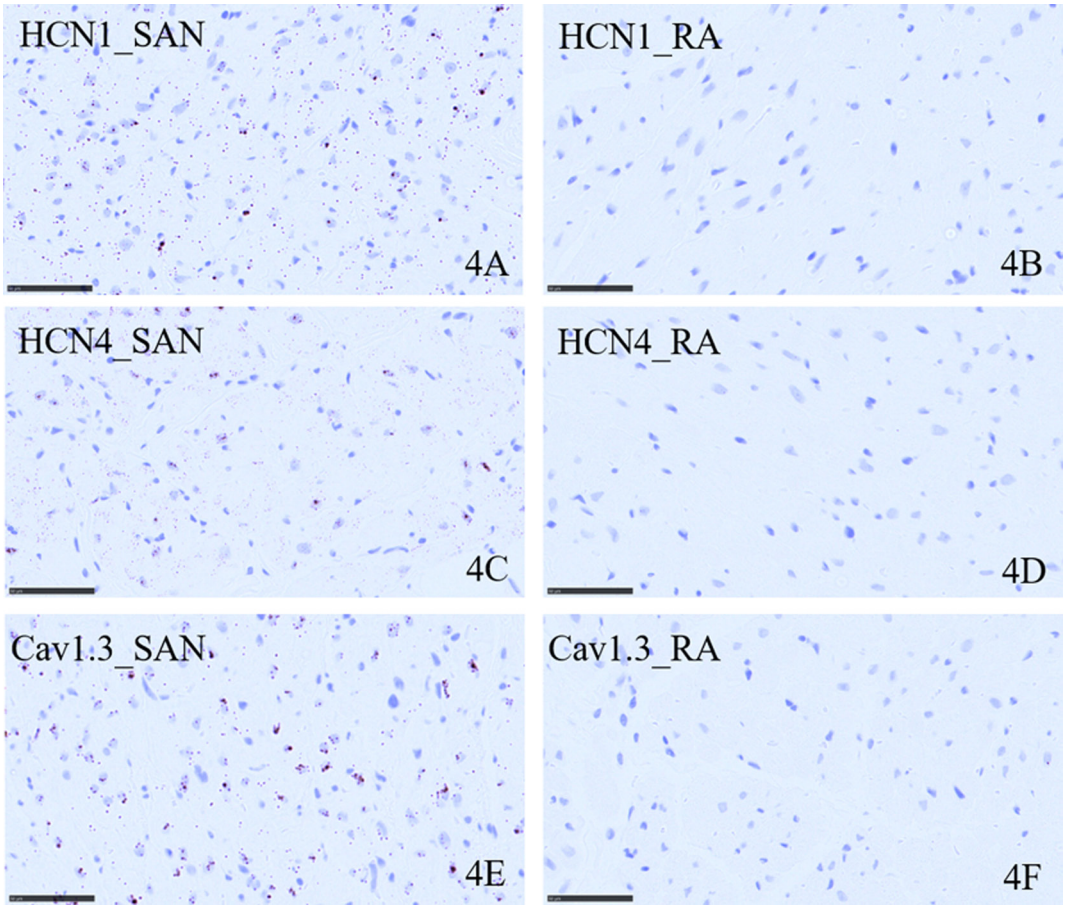

Fig. 4. Representative RNAscope staining photos of HCN1, HCN4, and Cav1.3 in a dog heart (bar: 50 µm). A: RNAscope HCN1 mRNA staining in the SAN (score: 2+), B: RNAscope HCN1 mRNA staining in the RA (score: 0), C: RNAscope HCN4 mRNA staining in the SAN (score: 2+), D: RNAscope HCN4 mRNA staining in the RA (score: 0), E: RNAscope Cav1.3 mRNA staining in the SAN (score: 2+), F: RNAscope Cav1.3 mRNA staining in the RA (score: 0). SAN: sinoatrial node; RA: right atrium.

Fig. 2. Individual gene expression scores of the hearts with RNAscope in monkeys (A) and dogs (B).

Fig. 3. Representative RNAscope staining photos of HCN1, HCN4, and Cav1.3 in a monkey heart (bar: 50 µm). A: RNAscope HCN1 mRNA staining in the SAN (score: 2+), B: RNAscope HCN1 mRNA staining in the RA (score: 1+), C: RNAscope HCN4 mRNA staining in the SAN (score: 3+), D: RNAscope HCN4 mRNA staining in the RA (score: 1+), E: RNAscope Cav1.3 mRNA staining in the SAN (score: 2+), F: RNAscope Cav1.3 mRNA staining in the RA (score: 0). SAN: sinoatrial node; RA: right atrium.

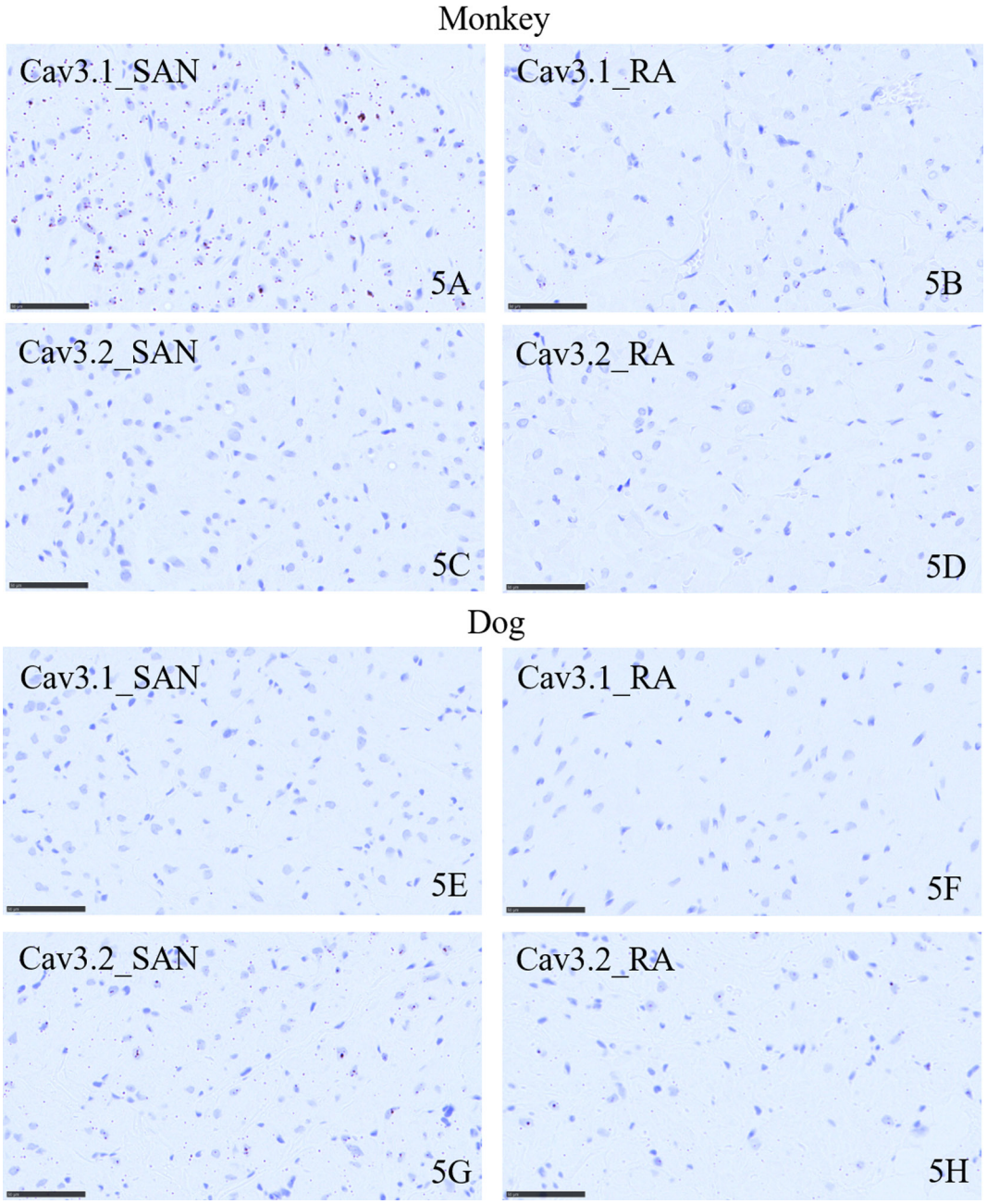

Fig. 5. Staining pattern of T-type voltage-gated calcium channels (Cav3.1 and 3.2) in dogs and monkeys (bar: 50 μm). A: RNAscope Cav3.1 mRNA staining in the SAN of a monkey (score: 2+), B: RNAscope Cav3.1 mRNA staining in the RA of a monkey (score: 1+), C: RNAscope Cav3.2 mRNA staining in the SAN of a monkey (score: 0), D: RNAscope Cav3.2 mRNA staining in the RA of a monkey (score: 0), E: RNAscope Cav3.1 mRNA staining in the SAN of a dog (score: 0), F: RNAscope Cav3.1 mRNA staining in the RA of a dog (score: 0), G: RNAscope Cav3.2 mRNA staining in the SAN of a dog (score: 1+), H: RNAscope Cav3.2 mRNA staining in the RA of a dog (score: 1+). SAN: sinoatrial node; RA: right atrium.

a dog heart (Fig. 6).

Discussion

In general, ion channels were expressed in the cell membrane, and mRNA expression was confirmed in the cytoplasm in the present study. Some dots were observed in the nucleus at various frequencies, which may indicate that the probe bound pre-mRNA in the nucleus due to the limitations of each probe size (approximately 50 bases) and detection method for RNAscope.

SAN-specific or predominant distribution was confirmed in the HCN1 (only in dogs), HCN4, and Cav1.3 mRNAs of dogs and monkeys. Notably, HCN1 and HCN4 mRNAs were exclusively expressed in the SAN in this study. In a previous report, human HCN1 mRNA was also

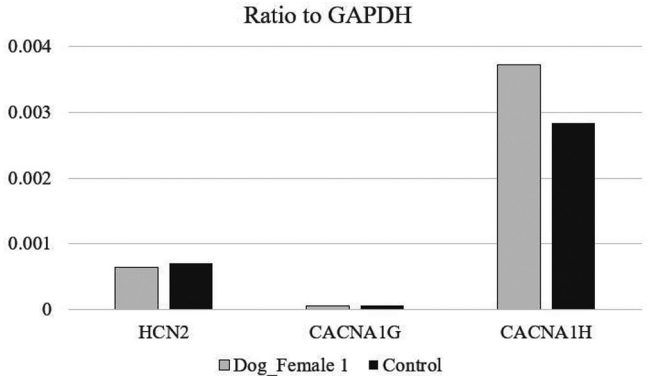

Fig. 6. Real time reverse transcription polymerase chain reaction of HCN2, CACNA1G (Cav3.1), and CACNA1H (Cav3.2) in formalin-fixed, paraffin-embedded (FFPE) dog heart (Dog_Female1) and commercially available dog heart (control) RNA samples. The data are presented as ratios to glyceraldehyde 3-phosphate dehydrogenase ($2^{-\Delta Ct}$). The relative expression level of the Cav3.2 gene was higher than those of the Cav3.1 and HCN2 genes in both the FFPE and control heart samples.

found to be a prevalent isoform in the SAN compared to the RA[7], indicating the similarity of the HCN1 mRNA expression profile in the SAN between dogs and humans. However, some reports showed that HCN1 mRNA was not detected in either region of the canine heart using RT-PCR[5, 6]. HCN4 and Cav1.3 mRNAs in humans were reported to be expressed predominantly in the SAN, although they were also detected in the RA[7]. In other targets, the expression levels of Kir3.1 and NCX1 in monkeys and Kir3.4 in dogs and monkeys were slightly higher in the SAN than in the RA. The previous human PCR data showed that the expression levels of Kir3.1 and NCX1 were also higher in the SAN, but that of Kir3.4 was not significantly different between the SAN and RA[7].

The T-type voltage-gated calcium channels (Cav3.1 and 3.2) showed different expression profiles between dogs and monkeys. In monkeys, the expression of Cav3.1 was observed in both the SAN and RA (slightly higher in the SAN), but Cav3.2 was not detected in either the SAN or RA. In contrast, canine Cav3.2 mRNA was equally detected in the SAN and RA, which was consistent with a previous report[8], but the expression of Cav3.1 mRNA was not confirmed in dogs using RNAscope. Our real time RT-PCR data from a dog FFPE section showed a similar profile using RNAscope, indicating higher expression of Cav3.2 compared to that of Cav3.1. Based on the present data, the mRNA expression level of Cav3.1 in dog FFPE sections may be below the lower limit of detection by RNAscope. In the human PCR data of the SAN and RA, Cav3.1 mRNA was at least 10-fold more abundant than Cav3.2 mRNA, which was below the detection threshold[7], indicating that human and monkey data showed similar profiles. Differences in the expression of T-type voltage-gated calcium channels in dogs and monkeys may be worth considering for the evaluation of CV effects in drug candidates that may affect these channels. The dysfunction of Cav3.1 channels is known to cause human congenital bradycardia and heart block[9].

Unlike the previously reported human and canine HCN2 expression levels in the SAN and RA[6, 7], HCN2 mRNA expression in dogs and monkeys was not detected by RNAscope. Real-time RT-PCR data generated using a dog FFPE section showed that the relative expression level of the HCN2 gene was lower than that of Cav3.2, which was only slightly detected by RNAscope in the present study. Therefore, the mRNA expression level of HCN2 in dogs may be low in the FFPE tissue and generally below the lower limit of detection by RNAscope.

In addition, Cav1.2, Kv11.1/ERG, and KvLQT1 were almost equally expressed in both the SAN and RA in both dogs and monkeys, and the expression patterns were nearly consistent with previous reports in dogs[6, 8]. Kv11.1/ERG mRNA expression levels in humans were higher in the RA than in the SAN, and Cav1.2 and KvLQT1 mRNA expression levels in humans were comparable in the SAN and RA[7].

To the best of our knowledge, there are limited reports on the mRNA expression patterns of ion channels in monkeys and dogs, and this is the first report to compare these expression patterns using RNAscope *in situ* hybridization. According to our data, the ion channels showed a complex and heterogeneous pattern of expression in the SAN and RA in dogs and monkeys. We believe that a detailed analysis of the potential contributor's mRNA expression in pacemaking of normal canine and monkey SANs may be of interest to readers, and the differences in mRNA expression patterns of the SAN and RA in each species may be useful for understanding the effect on automaticity of the heart in nonclinical studies as well as being relevant to humans.

Disclosure of Potential Conflicts of Interest: All authors are employees of Takeda Pharmaceutical Company Limited (Osaka, Japan).

Acknowledgments: The authors would like to thank Yumiko Miyamoto from Axcelead Drug Discovery Partners, Inc. for her excellent technical support with this work. We also thank Lisa Cicia from Takeda Pharmaceutical Company Limited for her assistance with language editing.

References

1. Boyett MR, Honjo H, and Kodama I. The sinoatrial node, a heterogeneous pacemaker structure. Cardiovasc Res. **47**: 658–687. 2000. [Medline] [CrossRef]
2. Huang H, Pugsley MK, Fermini B, Curtis MJ, Koerner J, Accardi M, and Authier S. Cardiac voltage-gated ion channels in safety pharmacology: Review of the landscape leading to the CiPA initiative. J Pharmacol Toxicol Methods. **87**: 11–23. 2017. [Medline] [CrossRef]
3. Aziz Q, Li Y, and Tinker A. Potassium channels in the sinoatrial node and their role in heart rate control. Channels (Austin). **12**: 356–366. 2018. [Medline] [CrossRef]
4. Wang F, Flanagan J, Su N, Wang LC, Bui S, Nielson A,

Wu X, Vo HT, Ma XJ, and Luo Y. RNAscope: a novel in situ RNA analysis platform for formalin-fixed, paraffin-embedded tissues. J Mol Diagn. **14**: 22–29. 2012. [Medline] [CrossRef]

5. Zicha S, Fernández-Velasco M, Lonardo G, L'Heureux N, and Nattel S. Sinus node dysfunction and hyperpolarization-activated (HCN) channel subunit remodeling in a canine heart failure model. Cardiovasc Res. **66**: 472–481. 2005. [Medline] [CrossRef]
6. Yeh YH, Burstein B, Qi XY, Sakabe M, Chartier D, Comtois P, Wang Z, Kuo CT, and Nattel S. Funny current down-regulation and sinus node dysfunction associated with atrial tachyarrhythmia: a molecular basis for tachycardia-bradycardia syndrome. Circulation. **119**: 1576–1585. 2009. [Medline] [CrossRef]
7. Chandler NJ, Greener ID, Tellez JO, Inada S, Musa H, Molenaar P, Difrancesco D, Baruscotti M, Longhi R, Anderson RH, Billeter R, Sharma V, Sigg DC, Boyett MR, and Dobrzynski H. Molecular architecture of the human sinus node: insights into the function of the cardiac pacemaker. Circulation. **119**: 1562–1575. 2009. [Medline] [CrossRef]
8. Gönczi M, Birinyi P, Balázs B, Szentandrássy N, Harmati G, Könczei Z, Csernoch L, and Nánási PP. Age-dependent changes in ion channel mRNA expression in canine cardiac tissues. Gen Physiol Biophys. **31**: 153–162. 2012. [Medline] [CrossRef]
9. Mesirca P, Torrente AG, and Mangoni ME. Functional role of voltage gated Ca(2+) channels in heart automaticity. Front Physiol. **6**: 19. 2015. [Medline] [CrossRef]